NASA TM X- *70794*

THE SURFACE GEOMETRY OF INHERITED JOINT AND FRACTURE TRACE PATTERNS RESULTING FROM ACTIVE AND PASSIVE DEFORMATION

MELVIN H. PODWYSOCKI

DAVID P. GOLD

JULY 1974

GSFC —— **GODDARD SPACE FLIGHT CENTER** ——

GREENBELT, MARYLAND

For information concerning availability
of this document contact:

Technical Information Division, Code 250
Goddard Space Flight Center
Greenbelt, Maryland 20771

(Telephone 301-982-4488)

ILLUSTRATIONS (Continued)

TABLES

THE SURFACE GEOMETRY OF INHERITED JOINT AND FRACTURE

TRACE PATTERNS RESULTING FROM ACTIVE

AND PASSIVE DEFORMATION

Melvin H. Podwysocki
Code 923
Goddard Space Flight Center

David P. Gold
Geosciences Department
The Pennsylvania State University
University Park, Pa. 16802

July 1974

THE SURFACE GEOMETRY OF INHERITED JOINT AND FRACTURE TRACE PATTERNS RESULTING FROM ACTIVE AND PASSIVE DEFORMATION

M. H. Podwysocki
D. P. Gold

ABSTRACT

The surface traces and trajectories of "joints" and "fractures" located over simple subsurface structures, with configurations optimized to a horizontal cylinder and vertical hemisphere and combinations thereof, are examined for two hypothetical methods of fracture development. The models are generated for a "rubber sheet" deformation and assume (a) that a fracture system may be inherited from the basement rocks through any overlying consolidated sediment, (b) that these fractures would be deformed by any subsequent movements in the basement rocks, (c) that in any kinematic folding, these fractures would be rotated and displaced by a flexural slip mechanism, and (d) that for supratenuous folds, any fractures developed during compaction would be focused through the center of curvature. It is asserted that (a) the inherited fractures, while being rotated and displaced by the bedding plane slip, would project vertically to the surface, i.e., orthographically, and (b) that fractures induced during compaction would converge upward in a down-warp or diverge in an upwarp from a focal point in the case of a dome or basin (periclinal structure) and a focal line for a supra-tenuous fold, and that these would project gnomonically to the surface. While the former mechanism is considered to be "active" and may be generated by local basement uplifts, the latter is "passive" and is typified by differential compaction of sediments over a reef core.

If these assumptions and assertions are accepted, then the attitude (strike and dip) of a deformed primary joint or fracture and its trajectory (vertical projection of its line of intersection with the deformed reference surface) can be used as indicators of subsurface structure. If a regular fracture grid is deformed, then fracture density and pattern become important diagnostic parameters. Various patterns of an initially orthogonal (square) fracture grid are modeled according to active and passive deformation mechanisms.

In the active periclinal structure with a vertical axis, fracture frequency (number/unit area) increases both over the dome and basin, and remains constant with decreasing depth to the structure. Active cylindrical folds with horizontal axes deform the initially orthogonal fracture grid, producing a grid trajectory pattern elongate in a direction parallel to the fold axis and causing a relative

increase in fracturing for that fracture direction forming the smallest angle to the structural axis. Where one of the fracture directions coincides with the structural axis, a rectangular pattern develops; rhomboid and rhombus patterns are produced for oblique intersections.

For passive periclinal features such as a reef or sand body with a reference grid on the unconformity, fracture frequency is determined by the arc of curvature and shows a reduction over the reef mound and an increase over the basin. In addition, depth to the structure also influences fracture frequency, causing a relative increase with increasing depth of erosion over a reef and a decrease for the basin. Passive cylindrical folds produce a grid pattern elongate in a direction perpendicular to the fold axis, with the fracture direction forming the largest angle to the structural axis being preferentially enhanced. The pattern is rectangular where the structural axis and one of the fracture directions coincide, and forms rhomboids and rhombuses where the two meet at oblique angles.

Decreasing the dihedral angle between the limbs of the structure further intensifies the changes in fracture frequency and grid shape of the fracture pattern.

CONTENTS

ILLUSTRATIONS

THE SURFACE GEOMETRY OF INHERITED JOINT AND FRACTURE TRACE PATTERNS RESULTING FROM ACTIVE AND PASSIVE DEFORMATION

INTRODUCTION

The use of joint or fracture patterns, as derived from ground observations or airborne remote sensing techniques, to depict subsurface geologic structure has had a long history and only mixed success. Studies of fracture patterns for the prediction of the hydrogeologic behavior of rock materials in groundwater and petroleum extraction programs have proved reasonably reliable and fruitful (Lattman and Parizek, 1964; Siddiqui and Parizek, 1971; Alpay, 1973). Blanchet (1957) and Gol'braikh et al., (1968a,b) applied fracture pattern analysis to detect "anomalies" useful in petroleum exploration. However, it has been applied in other areas with less success as an exploration tool (Henderson, 1960; Huntington, 1969; Rumsey, 1971). This may be due in part to non-standardization of techniques, differences in the tectonic regimes of the various study areas, and a lack of understanding of the possible mechanisms responsible for the observed fracture patterns. This is especially true where attempts are made to relate the fracture patterns to the structures responsible for entrapping the hydrocarbons (Huntington, 1969; Rumsey, 1971).

The object of this paper is to postulate several "deformation" mechanisms and to model the changes which may occur in the primary fracture patterns manifested as joints or fracture traces and which may occur over buried geologic structures in areas of essentially flat-lying sedimentary rocks, such as occur in oil and gas producing districts on the continental platforms.

RATIONALE

Fracture traces (Lattman, 1958) and their closely related synonyms (microfractures, Blanchet, 1957; mesofractures, Haman, 1964; megajoints, Gol'braikh et al., 1968a,b) have been noted on aerial photographs and topographic maps for the past several decades. These naturally occurring features, which manifest themselves as alignments of vegetation, dark soil tones, streams, topographic sags and combinations thereof, are unrelated to bedding and pose a geologic enigma. They are most commonly associated with zones of increased frequency of joints (Lattman and Nickelson, 1958; Lattman and Matzke, 1961; Lattman and Parizek, 1964; Gol'braikh et al., 1968a,b; Shul'ts, 1969), and although the definition (Lattman, 1958) restricts fracture traces to lengths less than 1.6 km, some longer linear features (lineaments) that are similar in expression have been mapped.

Although most workers agree that the majority of these linear features observed on aerial photographs are the surface trace of three-dimensional fractures generally having little or no apparent displacement, opinions vary on their relationship to other subsurface structures. One school of thought believes that a nearly one-to-one relationship exists between directions of jointing and fracture traces (Lattman and Nickelsen, 1958; Hough, 1959; Boyer and McQueen, 1964). These authors based their conclusions on observations in areas of nearly horizontal, relatively undisturbed sedimentary rocks. Another group of studies concluded that large discrepancies occur between directions of fracture traces and joints (Brown, 1961; Keim, 1962; Matzke, 1961). However, these studies were made in areas of deformed rocks (i.e., the folded Appalachian Mountains of Pennsylvania, porphyry copper stocks in Arizona, Llano Uplift of Texas). Lattman and Matzke (1961) suggested that in rocks dipping less than 5 degrees, fracture trace directions reflect primary jointing directions, whereas in more disturbed areas, fracture traces reflect fracturing associated with stresses responsible for the deformation. Because the directions of fracture traces and jointing coincide in platform areas, and because this study confines its results to those areas, either of the two features might be applicable to the discussion of the models in this paper.

Consistent, worldwide, nearly orthogonal fracture and joint patterns have been recognized in the Precambrian Shield areas and basement rock bodies of most continents (Hobbs, 1911; Henderson, 1960; Badgely, 1965). The cause of the "regmatic shear" net (Sonder, 1947) has not been totally agreed upon, however, in most minds its origin is related to global tectonic mechanisms such as rotational (Vening Meinesz, 1947) or shear forces (Moody and Hill, 1956). This basic "shear net" consists of components oriented in a north-south, east-west, northeast and northwest directions. In most cases all components are not equally developed (Shul'ts, 1969). On a mesoscopic scale, this effect can be noticed in outcrops as sets of nearly orthogonal and vertically dipping joints (Shul'ts, 1969).

Similar global patterns have been observed in the overlying sedimentary rock, and they appear to be propagated upward with time as an imposed or inherited pattern onto the younger cover rocks (Blanchet, 1957; Mollard, 1957; Henderson, 1960; Hodgson, 1961; Beloussov, 1962; Wobber, 1967; Wise, 1968). Blanchet (1957) and Hodgson (1961) suggest earth tide forces, which cause repeated diurnal stresses and induce failure along pre-existing zones of weakness, as a primary cause for the appearance of the basement fractures in the overlying rocks. Hodgson (1961) and Cook and Johnson (1970) believe these joints can form early in the history of a sedimentary unit, as planes of weakness formed during diagenesis. Kupsch and Wild (1955) and Badgely (1965) consider earthquakes and renewed tectonism as the propagating mechanism.

Some researchers have noted that this nearly orthogonal and conjugate set of fractures are normal to bedding even in deformed structures (i.e., anticlines) (Duschatko, 1953; Kelley, 1959; Kelley and Clinton, 1960). Because the patterns showed little or no geometric relation to the forces responsible for the structures, and because the pattern in the deformed rocks, when rotated back to horizontality was the same as the pattern located off the structure in horizontal strata, these authors concluded that the pattern existed prior to the deformation. It is this deformed fracture pattern, and its surface configuration, that may be an important factor for the isolation of such subsurface structures.

The key to an exploration program for buried structures using fracture analysis has been the recognition of inconsistencies or deviations from the global fracture pattern. Shul'ts (1969) suggests that those linears not related to the global pattern are due to local deformation. Blanchet (1957) claimed that by examining the fracture pattern as viewed on aerial photographs, he was able to find inhomogeneities (reefs) in the stratigraphic column by the use of "structural intensities". Saunders (1969) and Gol'braikh et al., (1968a, b), amongst others, also used fracture frequency (number of fractures per unit area) as determined from aerial photographs, to isolate buried anticlinal structures. The following discussion uses models to examine the rationale behind these purported exploration techniques.

ASSUMPTIONS AND ASSERTIONS

Some assumptions and assertions are made concerning joint and fracture development in the cover rocks overlying subsurface structural features. The assumptions are: (a) that in certain situations the cover rocks will inherit the fracture or joint pattern (frequency and orientation) from the underlying bedrock, particularly from the basement rocks; and (b) that during compaction of sedimentary rocks, any bedrock topography will influence the fracture or joint system developed. The consequences of these suppositions are examined for two different mechanisms of transmitting these "fracture" systems to the earth's surface. The mechanisms of upward projection of these fractures are based on the following assertions: (1) that if the strata with an inherited fracture system are deformed by flexural slip associated with subsurface buckling (folding), then the fractures will be displaced towards the areas of flexure and will overlie vertically the same fracture at depth; (2) that for a similar grid draped over subsurface topographic features (e.g., reef), the fracture pattern would radiate from the center of curvature during compaction and the formation of supratenuous folds.

The method of drawing the inherited fracture, distorted by subsurface faulting and flexural slip folding, is by projecting the displaced fracture surfaces orthographically to the surface (see Figures 1 and 2). The resultant flexures are kinematic folds, and the structure is considered to be "active". The intersections

between fractures are used as control points; their positions and attitude after deformation are projected to the earth's surface and the trace of the now curved fracture surfaces is completed along the trajectories between the control points (see Figure 2). For supratenuous folds, which are considered to be "passive", the control grid is projected gnomonically to the earth's surface from the center or center line of curvature for the various subsurface configurations (see Figure 3).

If these assumptions and assertions are accepted, then the distortion of a square control grid is characteristic of the mechanics and amount of deformation. The following diagrams are presented to illustrate the changes in pattern of a square control grid at various orientations to a flexure axis and with increasing degrees of deformation as indicated by a decrease in the axial or dihedral angle between the flexed limbs. Deflection of the fracture planes and distortions in the grid pattern as seen on the earth's surface are characteristic of the method of projection, the initial geometry, and the amount of deformation. These patterns therefore may be diagnostic of subsurface structures of economic importance, provided they are not masked out by additional fractures induced by deformation. This type of analysis would most probably be applied in those rocks in which the flexures are gentle.

An initial square "joint" pattern, perpendicular to bedding in horizontal strata, will be distorted linearly and curvilinearly as a result of deformation. The amount of distortion will depend on:

(a) amount of deformation (i.e., the dihedral angle between the limbs of the fold, or the apical angle of the periclinal structure) and the shape of the fold,

(b) angle between the axial line of the fold and the strike of the joint directions and

(c) method by which the fracture is propagated to the surface.

Two models are considered in order to examine the nature of distortion based respectively on a flexural slip (kinematically active), and compaction (kinematically passive) mode of deformation. The models are generated to depict the shape and orientation of a regular (square) pattern of fractures or joints in stratified cover rocks as a result of active and passive sub-cover rock structures.

The shapes of the structures considered are (1) a horizontal cylinder (anticline and syncline) with its axis oriented parallel, 30°, 45°, 60° and 90° to the joint or fracture set, and (2) a dome and basin (periclines) with a vertical axis. Various combinations can be put together to simulate elliptical subsurface structures.

4

DISCUSSION OF MODELS

The following set of figures shows some generalized examples for different structural culmination angles and orientations of the original fracture set to the structure. Lithology and bed thickness also may affect the fracture patterns (DeSitter, 1964), especially if they are inclined. Therefore, in these examples we consider a rock mass that is homogeneous in lithology and bed thickness. We are concerned here with the reorientation of existing joints or fractures during or after deformation and their possible propagation through any cover rocks. If all the strata have been kinematically active, then a flexural slip mechanism may have operated between the beds, and the fractures are likely to be rotated and displaced, in essentially vertical zones (Figure 1). The horizontal displacement will represent the amount of crustal shortening if other forms of strain relief are neglected.

The initial vertical planar fractures, oblique to the fold axis, will be distorted in an elastic-sheet type deformation into curved surfaces, whose dip and strike will vary continuously between the crest and trough positions (see Figure 2). The line of intersection between this curved fracture surface and the folded reference bed is sketched in as a curvilinear trajectory. The strike and dip of the midpoint tangent plane and the plunge of the line are shown in Figure 2a, (points Y and Z) and its surface trace in Figure 2b. The plan views of these trajectories are illustrated in Figures 5-9, and thus they represent the surface traces projected orthographically from the reference bed.

Expanding on the assertions concerning supratenuous folds, a regular grid at the interface between buried topography, such as mounds or ridges of reefs, and the overlying sediments is likely to be propagated gnomonically upward during compaction (see Figure 3b). Thus the surface traces depicted in Figures 3, 10, and 11 are the direct surface intersections of hypothetical fractures propagated gnomonically from a focal point or line outward through the grid.

If undeformed strata above an unconformity have the ability to couple with the sub-unconformity fractures, then the sub-unconformity fracture pattern should be propagated to the surface by the action of earth tides. The sub-unconformity pattern should project to the surface relatively undistorted if the upper strata dip gently (see Figure 4). Areal positions will be displaced as a function of depth to the unconformity and dip of the upper beds:

$$\text{Axial Displacement} = d \times \text{Tan } \theta$$

where

d = depth to the axis as projected on the unconformity

θ = dip angle of overlying sediments.

5

DEFORMATION OF INHERITED FRACTURE PATTERNS

Consider the active flextural slip fold development in a competent bed with a pre-existing vertical joint or fracture set (Figures 5-9). The drawings in each figure depict folds of increasing deformation, quantified in terms of the dihedral angle between the limbs. The plan view of the initial state is shown on the left; progressively to the right folds with dihedral angles of 150°, 120°, and 90° are illustrated both for the anticlinal case (upper set) and synclinal case (lower set). Separating the plan view diagrams are the right sections (cross sections perpendicular to the fold axis). In Figures 6-9 a single right section is used; view to top of page for the anticline and the bottom of the page for the syncline. Strike and dip measurements of the plane are given as well as the inclination and direction of the joint trajectory lines for oblique intersections of fractures and structural axes. The strike and dip of the fracture plane and trajectory lines for midway on the limbs are listed in Table 1 for fold dihedral angles up to 60°. All but the open and gentle folds are likely to develop secondary fracture planes as a result of deformation and may be indicated by zones of increased fracturing.

Joints and fractures parallel and perpendicular to the fold axis are the least affected (Figure 5). The parallel joints are rotated out of the vertical through the dip angle about the axis of the fold, and are displaced toward the fold axis proportional to the amount of dip rotation (note decrease in interval AA' with increasing deformation). The fracture directions normal to the fold axis show no apparent motion. It is obvious that there is no displacement of a plane along the fold axis of a single fold, but there will be displacement between adjacent fold axes. The results are:

(a) an increase in fracture frequency about the axis of curvature, and

(b) a distortion of the initial square grid to a rectangular grid elongate in the direction of the fold axis. Note that none of the lines are deflected.

For joints or fractures striking at an angle of 45° to the fold axis (Figure 6), there is no reduction in the length between intersections parallel to the fold axis. The effect of rotating these vertical fracture planes about the fold axis is to progressively increase the angle between the fracture strike and the fold axis, with increasing dip. In the limiting case of an isoclinal fold (90° rotation) the strike would be perpendicular to the fold axis. However, the fracture plane will change dip from vertical on the axes of the crest and trough (where the original attitudes are preserved) to inward dipping (anticline), or outward dipping (syncline) on the limbs. The plunge of the trajectory line is shown by the arrow and inclination.

The fracture intersections are displaced perpendicular to the fold axis by a distance proportional to the dip angle, and there results:

(a) a distortion of the original square grid to an irregular rhombhoidal pattern elongate in the direction of the fold axis,

6

(b) the fracture lines are sigmoidal rather than straight as a consequence of a changing dip inward from crest to flank for the anticline or outward from trough to flank for the syncline, and

(c) the dihedral angle between conjugate fracture sets as viewed in plan becomes progressively more acute in the direction of the fold axis, as the fold dihedral decreases (increased deformation).

In Figure 7 (top) the northeasterly fracture set of the initial square grid makes an angle of 30° to the fold axis and the northwesterly set an angle of 60°. The lower diagrams are set up in a similar way to those in Figure 5 and 6, except that the angle for the northeasterly and northwesterly sets are reversed to show that the converse case is a mirror image of the former. Although the initial strike and dip angles are preserved on the anticlinal and synclinal axial lines, both sets are rotated inward on the flanks of the anticline or outward with respect to the synclinal axis, but the value of strike and dip as well as trajectory lines vary (see Table 1). The angle between the strike of those fracture planes on the flanks and the fold axis increases with decreasing dihedral angle of the fold. The fracture intersections are no longer symmetrical about the fold axis; with differential displacement proportional to the dip angle and perpendicular to the fold axis there results:

(a) differential distortion on the two sets of fractures into an irregular parallelogram with its long axis elongate in the direction of the fold axis,

(b) sigmoidal fracture lines, and

(c) the fracture direction with the smallest angle to the fold axis will have the greatest frequency and density of fractures per unit area.

Periclinal structures are depicted in Figure 8. Because of their axial symmetry two different grid spacings are considered: the upper shows a closer spaced grid over a dome; the lower illustrates a wider grid over a basin. By reversing the dip direction these diagrams may be converted to their opposite forms. Peripheral distortions are severe because of the radial displacement. In nature, the strain is likely to be accommodated over the whole structure and fracture trace trajectories with gentler curves would be expected.

The inward displacement of all curves toward the vertical axis of the periclinal structure results in

(a) a greater density of fractures over the structures,

(b) sets of intersecting concave patterns, with the degree of distortion of the fracture trajectory increasing with decreasing apical angle (increased deformation), and

7

(c) the original grid is distorted into irregular trapezoids with greater distortion on the flanks of the fold.

(d) grid distortion is such that the acute dihedral angles between the planes are bisected by radial lines.

In all cases considered, the nature of the curvature of the crests or troughs of the structure are optimized smooth curves about intersecting straight lines (see Figures 5-8). If the crest or trough is gently curved or flat, there will be little modification of the original grid and most of the changes in density and direction will take place over the flanks. In Figure 9, part of a box fold* and a monocline are shown. In both cases, any joints parallel to the fold axis will dip only in one direction. For the monocline, these will be one side of the anticline considered in Figures 5-7 (only the 45° case is given).

As the dip of the reference bed becomes more extreme, secondary fractures will be developed and complicate the fracture pattern, particularly in the hinge zones. For a box fold, initial fractures parallel to the fold will not intersect the surface (see Figure 9b). For oblique orientations of the initial grid to the fold axis, the strike of the fractures will be rotated perpendicular to the fold axis (see Figure 9c and d). The dip of the fractures will correspond to its initial angle to the fold axis, and its intersection with the reference bed (trajectory) will coincide with the dip line of the fracture plane. If the fracture "planes" are projected to the surface, the 45° grid will be rotated to strike perpendicular to the fold axis, producing a regular undistorted square grid over the flat-lying margin, distorted rhombohedrons over the axis, and elongate rectangles between the flexural axes, with the direction of elongation perpendicular to the fold axes. The grid oriented 60-30° to the fold axes will produce a somewhat similar pattern but with less symmetry. Likewise the trace of the fractures between the flexural axes will have a rectangular pattern, elongate perpendicular to the fold axes with inward dips of respectively 60° and 30°.

Gol'braikh et al., (1968b), show numerous examples of increased megajointing occurring over the crests of uplifts in the Vilyuisk Syneclise. In addition, on some of the small structures, they note that megajointing increased along the limbs of the structure. They claim that maximum fracturing intensity will occur in the area of maximum bending of the strata. Moreover, they show that several elongated uplifts whose axes parallel the regmatic shear net, have an increased number of megajoints parallel to their long axes. This may be analogous to the examples illustrated in Figure 4, where fractures parallel to the axis of uplift

---

*Maximum rate of strata curvature on the flanks of the structure.

will be preferentially enhanced. Dranovskii (1970) notes that maximum fracturing will occur on the crest of ridge-like uplifts, whereas it develops along the limbs of box-like uplifts. Little information is given for the subsurface structural setting for the above cited examples and it may be argued that the observations simply indicate secondary deformation, however, the discussed mechanism may also play a role in the manifestation of these structures.

PROPAGATION OF FRACTURE PATTERNS ABOUT A FOCAL LINE OR POINT

The "passive" structure, about which overlying beds are draped by compaction, focuses fracture activity and may be analogous to magmatic pressure in plutons which cause the formation of cone sheets along the maximum principal stress trajectories and ring dikes along the maximum shear stress trajectories (see Anderson, 1936).

The construction of these (Figures 10 and 11) involves a non-kinematic syncline (elongate trough) and anticline (elongate ridge) side by side, with plan views on several levels or data planes. The center of curvature is determined by the dihedral or apical angle of the structure; evenly spaced points along the limbs represent the fracture plane intersections. In effect, these are handled by a form of gnomonic projection. The circular mound (dome) and depression (basin) are true gnomonic projections.

The effects on Figures 10 and 11 are similar (note: the 0-90° grid and the 45° grid are projected simultaneously for Figure 10). Depending on the datum level, there is generally a convergence of the fracture traces parallel and at an angle to the fold axis over the trough, and a divergence over the ridge. The inclined grids are progressively distorted from small irregular rhombohedrons elongated in the direction of the fold axis over the troughs, to large irregular rhombohedrons elongate perpendicular to the axis over the ridges.

The trace of an initial grid over a buried dome is complex and should follow telescoped, strongly concave grid sets over a depression and conversely, convex grid sets over a dome (as illustrated in Figure 11).

These models are consistent with the results of Blanchet (1957), where he shows that "structural intensity" (amount of fracturing) is minimal over a local reef proper and greater along the reef margins. Rumsey (1971), in his limited success in exploring for characteristic fracture patterns over reefs, indicates that at least one reef had a greater concentration of fractures along a portion of its periphery. John Rich (Lattman, 1969, pers. com.) used the existence of basalt capped buttes isolated from a retreating scarp in eastern New Mexico as an exploration tool for buried lenticular sands. Rich hypothesized some deflecting mechanism for the

9

fracture pattern, thereby more intensely fracturing the surrounding mesa cap-
rock and increasing its susceptibility to erosion. Podwysocki (1974) found a
paucity of fracture traces in the vicinity of several reef structures, after ex-
traction of a regional or background value using trend surface analysis.

SUMMARY AND CONCLUSIONS

The dominant joint sets present in platform areas are most likely due to a global
regmatic shear pattern. This pattern may be passed from the basement into the
overlying horizontal sediments with little alteration. The development of an un-
conformity could cause a change in the position of the pattern into the sediments
overlying the unconformity. Although several limiting factors exist, it may be
possible to detect this change in pattern and apply it in oil and gas exploration.

In the quest for detecting subsurface structure from the fracture or joint patterns,
which may be influenced by the structures and propagated to the surface, two
hypothetical models are considered. The first is termed active and involves
kinematic structures with flexural slip; even with rotation to alter the dip, the
fracture is projected vertically with an adjustment in position proportional to the
amount of crustal shortening.

The second is termed passive and involves an updip projection from a focal point
or line (the center of curvature) to the surface. This is the mechanism thought
to propagate outward from compaction folds. While there is no hard proof for
either process, there is a considerable body of circumstantial evidence which
suggests these may be viable mechanisms. Probably these mechanisms may
represent two end members of a spectrum that may be continuous.

The patterns result from a combination of grid orientation, apical angle of domes
and basins, and dihedral angles of folds, and while there are small deviations in
fracture trajectories over buried structures (active and passive), these may be
difficult to detect in discontinuous joint or fracture trace lines.

Deflections seem to be the most sensitive indicators, but unfortunately, for
gently dipping structures the deflection angle may be of the same order as the
error of measuring orientation off aerial photographs. The dihedral angle be-
tween conjugate sets of fractures may be the best practical parameter to use.
Supporting this parameter should be fracture density and frequency and the shape
and direction of distorted grid. If the ambient grid pattern is known, then some
semiquantitative deduction could be made with reference to the models, e.g., a
zone in which all fracture traces are subparallel and perpendicular to the zone
axis, may represent the limb of a box fold.

ACKNOWLEDGMENTS

REFERENCES

Alpay, O. A., 1973, Application of aerial photographic interpretation to the study of reservoir natural fracture systems. Jour. Petroleum Technol., V. 25, No. 1, p. 37-45.

Anderson, E. M., 1936, The Dynamics of the Formation of Cone-Sheets, Ring-Dykes and Cauldron Subsidences; Proc. Roy. Soc. Edinburgh, V. 56, p. 128-163.

Badgely, P. C., 1965, Structural and Tectonic Principles; Harper & Row, New York, 521 p.

Beloussov, V. V., 1962, Basic Problems of Geotectonics, McGraw-Hill, 820 p.

Blanchet, P. H., 1957, Development of fracture analysis as an exploration method; Bull. Amer. Assoc. Petrol. Geol., V. 41, No. 8, p. 1748-1759.

Boyer, R. E. and J. E. McQueen, 1964, Comparison of mapped rock fractures and airphoto linears; Photogramm. Engineering, V. 30, No. 4, p. 630-635.

Brown, C. W., 1961, Comparison of joints, faults and airphoto linears; Bull. Amer. Assoc. Petrol. Geol., V. 45, No. 11, p. 1888-1892.

Cook, A. C. and K. R. Johnson, 1970, Early joint formation in sediments; Geol. Mag., V. 107, No. 4, p. 361-368.

DeSitter, L. U., 1964, Structural geology, 2nd ed.; McGraw-Hill, New York, 587 p.

Dranovskii, Ya. A., 1970, Morphological-structural analysis of the Lower Anadyr Depression; Geomorphology, No. 3, p. 234-240.

Duschatko, R. W., 1953, Fracture studies in the Lucero Uplift; U. S. Atomic Energy Comm. Rpt. RME-3072, 49 p.

Gol'braikh, I. G., V. V. Zabaluyev, A. N. Lastochkin, G. R. Mirkin, and I. V. Reinin, 1968a, Morfostrukturnye metody izucheniya tektoniki zakrytykh platformennykh neftegazonosnykh oblastei (Morphostructural methods for the study of tectonics in covered platform oil and gas bearing regions); NEDRA, 151 p.

Gol'braikh, I. G., V. V. Zabaluyev and G. R. Mirkin, 1968b, Tectonic analysis of megajointing: a promising method of investigating covered territories; Internat. Geol. Rev., V. 8, No. 9, p. 1009-1016.

Haman, P. J., 1964, Geomechanics applied to fracture analysis on aerial photographs; West Canadian Research Publ. of Geology and Related Sciences, Ser. 2, No. 2, 84 p.

Henderson, G., 1960, Air-photo lineaments in Mpanda area, Western Province, Tanganyika, Africa; Bull. Amer. Assoc. Petrol. Geol., V. 44, No. 1, p. 53-71.

Hobbs, W. B., 1911, Repeating patterns in the relief and in the structure of the land; Bull. Geol. Soc. Amer., V. 22, No. 1, p. 123-176.

Hodgson, R. A., 1961, Regional study of jointing in Comb-Ridge-Navajo Mountain area, Arizona and Utah; Bull. Amer. Assoc. Petrol. Geol., V. 45, No. 1, p. 1-38.

Hough, V. N. D., 1959, Joint orientations of the Appalachian Plateau in southwestern Pennsylvania; M. S. Thesis, The Pennsylvania State Univ., 82 p.

Huntington, J. F., 1969, Methods and applications of fracture trace analysis in the quantification of structural geology; Geological Magazine, V. 106, No. 5, p. 430-451.

Keim, J. W., 1962, Study of photogeologic fracture traces over the Bisbee Quadrangle, Arizona; M. S. Thesis, The Pennsylvania State University, 42 p.

Kelley, V. C., 1959, Origin of fractures in sedimentary rocks; Amer. Assoc. Petrol. Geol. Rocky Mtn. Record, Feb., 1959, p. 61-67.

Kelley, V. C. and N. J. Clinton, 1960, Fracture systems and tectonic elements of the Colorado Plateau; Univ. New Mexico Publ. in Geology, No. 6, 104 p.

Kupsch, W. O. and J. Wild, 1955, Lineaments in the Avonlea Area, Saskatchewan; Bull. Amer. Assoc. Petrol. Geol., V. 42, No. 1, p. 127-134.

Lattman, L. H., 1958, Technique of mapping geologic fracture traces and lineaments on aerial photographs; Photogrammetric Engineering, V. 24, No. 4, p. 568-576.

Lattman, L. H. and R. H. Matzke, 1961, Geologic significance of fracture traces; Photogrammetric Engineering, V. 27, No. 3, p. 435-438.

Lattman, L. H. and R. P. Nickelsen, 1958, Photogeologic fracture trace mapping in the Appalachian Plateau; Bull. Amer. Assoc. Petrol. Geol., V. 42, No. 9, p. 2238-2245.

Lattman, L. H. and R. R. Parizek, 1964, Relationship between fracture traces and the occurrence of groundwater in carbonate rocks; Jour. Hydrology, V. 2, No. 1, p. 73-91.

Matzke, R. H., 1961, Fracture trace and joint patterns of western Centre County, Pennsylvania; M. S. Thesis, The Pennsylvania State Univ., 39 p.

Mollard, J. R., 1957, Aerial mosaics reveal fracture patterns on surface materials in southern Saskatchewan and Manitoba; Oil in Canada, August 5, 1957, p. 26-50.

Moody, J. D. and M. J. Hill, 1956, Wrench fault tectonics; Bull. Geol. Soc. Amer., V. 67, No. 9, p. 1207-1246.

Podwysocki, M. H., 1974, An analysis of fracture trace patterns in areas of flat-lying sedimentary rocks for the detection of buried geologic structure; NASA-Goddard Space Flight Center Document X-923-74-200, 88 p.

Rumsey, I. A. P., 1971, Relationship of fractures in unconsolidated superficial deposits to those in the underlying bedrock; Modern Geol., V. 3, p. 25-41.

Saunders, D. F., 1969, Airborne sensing as an oil reconnaissance tool; in Unconventional Methods in Exploration for Petroleum and Natural Gas (Heroy, W. B., editor), Southern Methodist Univ., p. 105-125.

Shul'ts, S. S., 1969, Nekotorye voprosy planetarnoi treshchinovatosti i svyazannykh s neyu yavlenii (Some aspects of planetary jointing and related phenomena); Vestnik Leningrad. Univ., No. 1, p. 86-89.

Siddiqui, S. H. and R. R. Parizek, 1971, Hydrogeologic factors influencing well yields in folded and faulted carbonate rocks in central Pennsylvania; Water Resources Research, V. 7, No. 5.

Sonder, R. A., 1947, Discussion of "Shear patterns of the earth's crust" by F. A. Vening-Meinesz; Trans. Amer. Geophys. Union, V. 28, No. 6, p. 939-946.

Vening-Meinesz, F. A., 1947, Shear patterns of the earth's crust; Trans. Amer. Geophys. Union, V. 28, No. 1, p. 1-61.

Wise, D. U., 1968, Regional and sub-continental sized fracture systems detectable by topographic shadow techniques; in Conf. on Research in Tectonics (Kink Bands and Brittle Deformation) (Baer, A. J. & Norris, D. K., eds.), Geol. Surv. Canada Paper 68-52, p. 175-199.

Wobber, F. J., 1967, Fracture traces in Illinois; Photogrammetric Engineering, V. 33, No. 5, p. 499-506.

BASEMENT ROCKS

REFERENCE BED

FRACTURE TRAJECTORY (TRACE OF FRACTURE
PLANE INTERSECTION WITH REFERENCE BED)

TRACE OF FOLD AXIS

AA - A'A'   CRUSTAL SHORTENING
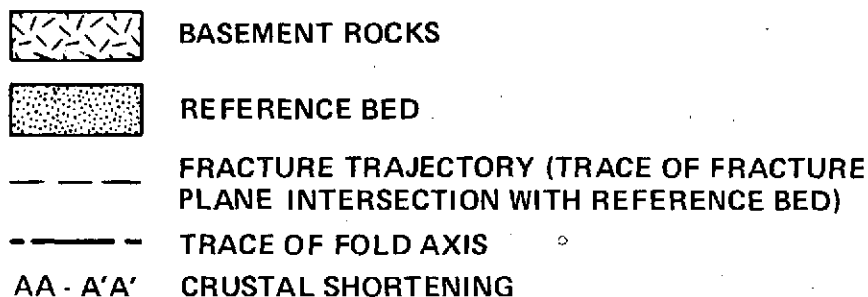
Figure 1. Block diagrams illustrating "rubber sheet" defor-
mation of an inherited vertical and orthogonal fracture pattern,
where fractures strike normal and parallel to the fold axis,
during flexural slip folding. (a) Fractures developed in cover
rocks by upward propagation of a basement fracture set. (b)
Post-deformation attitude and position of the inherited fracture
set. Arching is accompanied by a crustal shortening as indi-
cated by the difference between distance AA and A'A' and is
also shown as an apparent decrease in the width spacing
between those fractures paralleling the fold axis.

(a)

(b)

	REFERENCE BED
— — —	FRACTURE TRAJECTORY (TRACE OF FRACTURE PLANE INTERSECTION WITH REFERENCE BED)
▪-━━▪-	TRACE OF FOLD AXIS
F ━━ L	FOLD LINE
✛	VERTICAL FRACTURE PLANE INTERSECTION
21	STRIKE AND PLUNGE OF TRAJECTORY
▲60	STRIKE AND DIP OF FRACTURE PLANE
φ	DIHEDRAL ANGLE OF FOLD; 0 = 120°
NOP	INITIAL POSITION OF VERTICAL FRACTURE PLANES
NO'P	POSITION OF WARPED FRACTURE "PLANES"
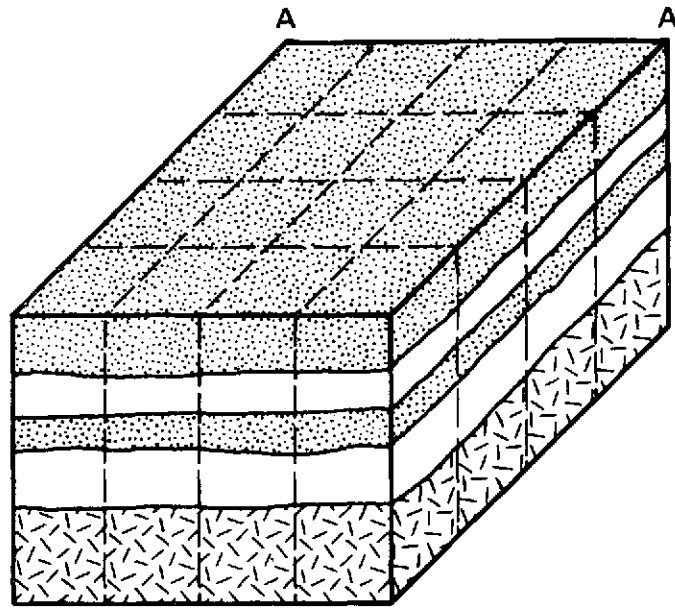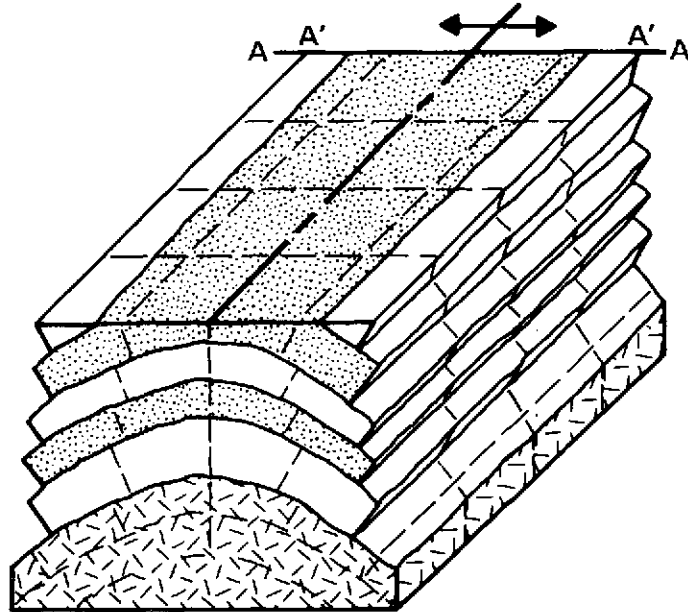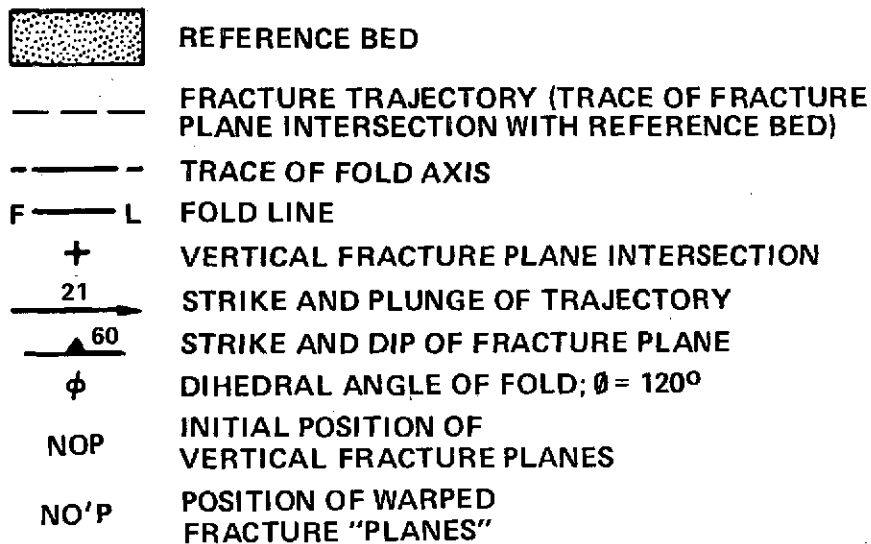
Figure 2. Diagrams illustrating "rubber sheet" deformation of an inherited vertical and orthogonal fracture grid striking oblique to the fold axis. (a) Block diagram showing the curved nature of the fracture surface between the crest and trough positions of the fold. The "lineations" on the fracture surface show the changes in attitude which occur along the fracture surface. This is quantitatively illustrated by the strike and dip symbols at points Y and Z on the reference surface (top of stipled bed). The arrows represent the surface trace of the trajectory or attitude of the intersection of the fracture plane and the reference surface at these points. (b) Plan view of the surface traces of the fracture net, both before and after deformation.

(a)

(b)

BASEMENT ROCKS

REEF

— — — FRACTURE TRAJECTORY (TRACE OF FRACTURE
PLANE INTERSECTION WITH REFERENCE BED)

O ,   CENTER OR AXIS OF CURVATURE

BAC   CYLINDRICAL UNCONFORMITY

Z   SURFACE TRACE OF SQUARE GRID AT THE
CYLINDRICAL UNCONFORMITY
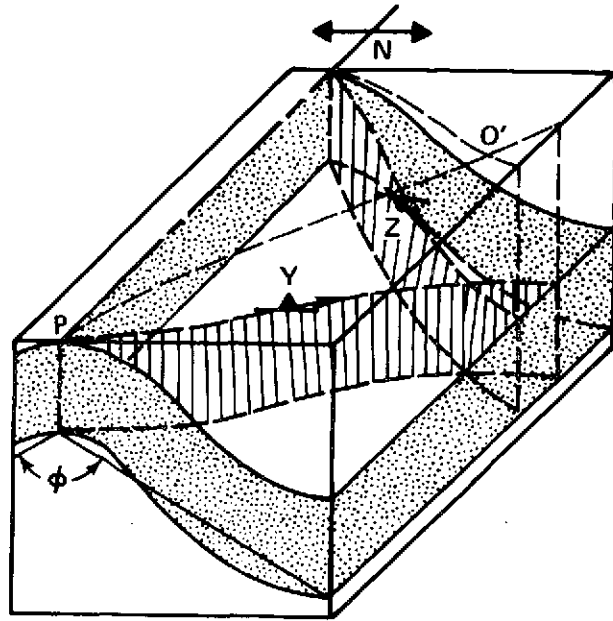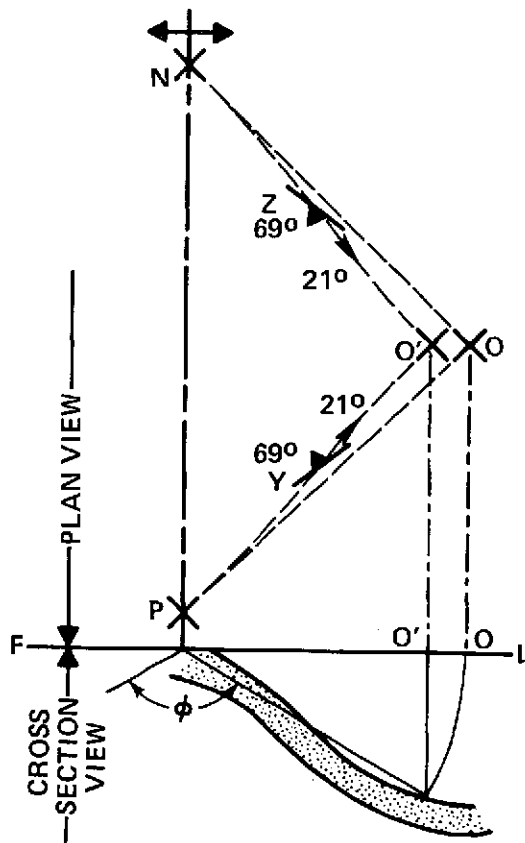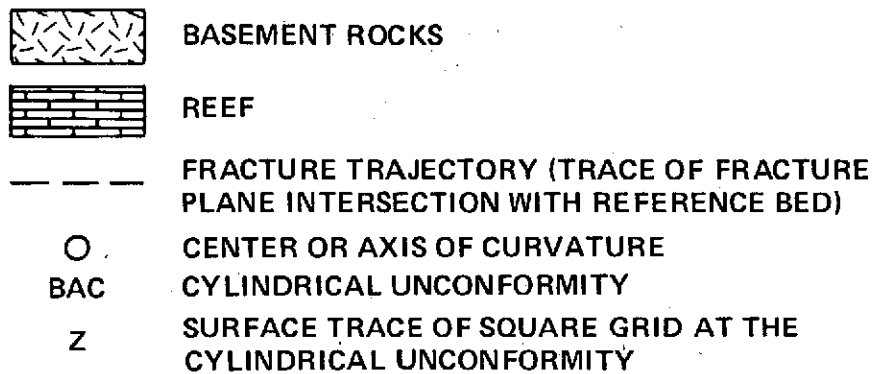
Figure 3. Block diagrams illustrating the hypothetical forma-
tion of fractures during compaction and the development of
supratenuous folds. (a) Unconsolidated sediments over a bed-
rock ridge, e.g., reef. (b) Trace of a regular (square) grid
at the unconformity projected through the center of curvature
(gnomonic projection) to the surface of the earth.
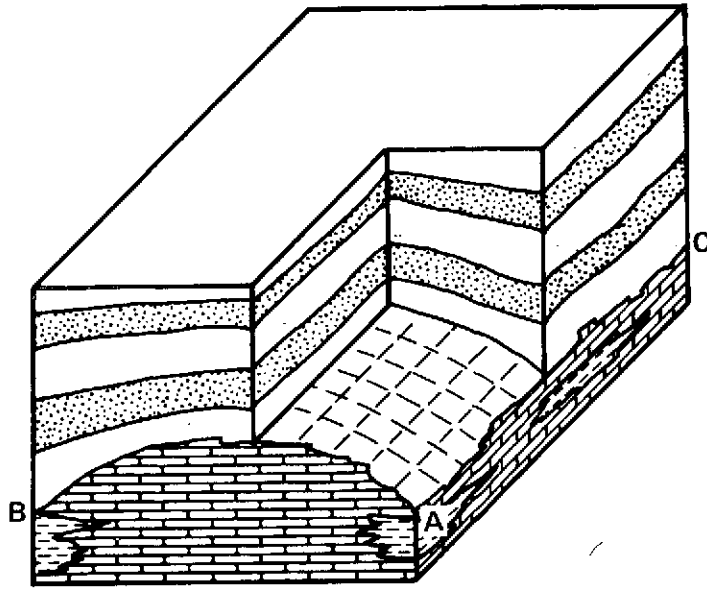
(a)
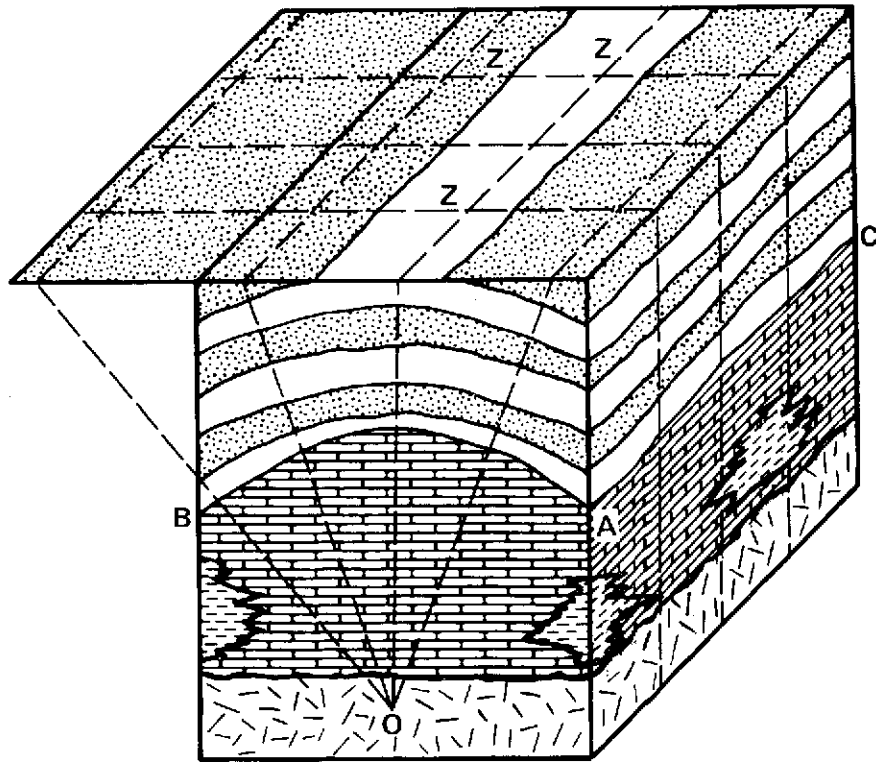
(b)
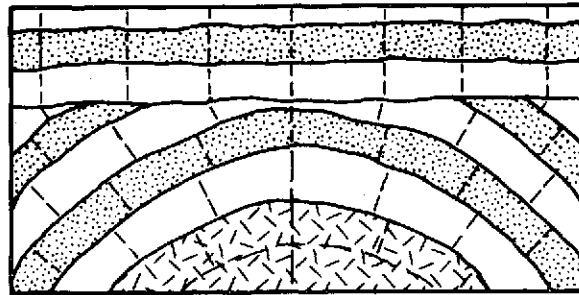
(a)
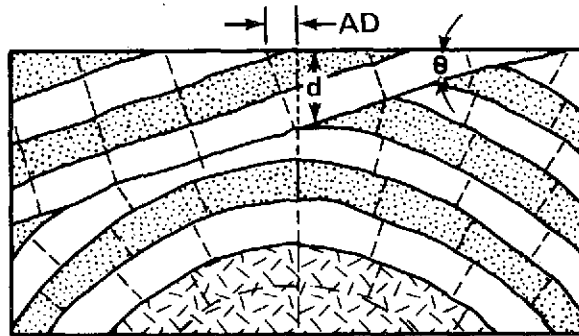
(b)

- - - FRACTURE TRAJECTORY (TRACE OF FRACTURE
       PLANE INTERSECTION WITH REFERENCE BED)
   d   DEPTH TO FOLD AXIS
  AD   AXIAL DISPLACEMENT
   θ   DIP ANGLE OF ROCKS

Figure 4. Cross sectional views of fracture patterns inher-
ited by the cover rocks through an angular unconformity. (a)
Horizontal upper beds. (b) Tilted upper beds. The displace-
ment of the sub-unconformity fold axis is a function of depth
to the unconformity and the dip of the upper beds and is given
by the formula AD = d x Tan θ.

REFERENCE BED

FRACTURE TRAJECTORY (TRACE OF FRACTURE
PLANE INTERSECTION WITH REFERENCE BED)

TRACE OF FOLD AXIS

$\blacktriangle$ 60   STRIKE AND DIP OF FRACTURE PLANE

ϕ DIHEDRAL ANGLE OF FOLD

F_____L   FOLD LINE

$+$ VERTICAL FRACTURE PLANE INTERSECTION
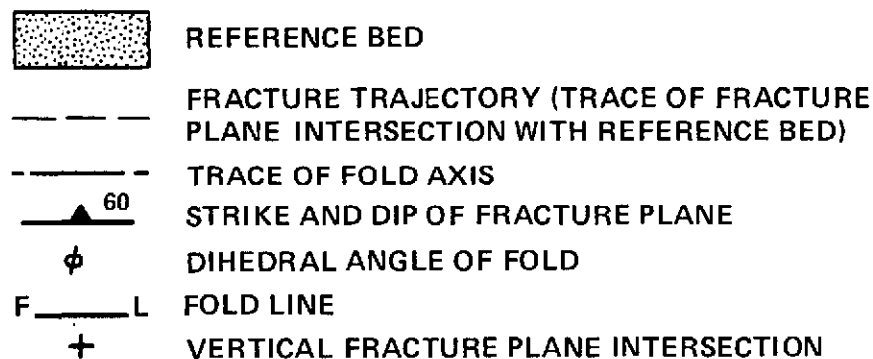
Figure 5. Surface traces of an original square, vertical fracture grid projected vertically from its intersec-
tion with the top of the folded reference bed. The initial state is shown on the left with the square grid oriented
0° and 90° to the fold axis. Progressively increasing deformation is indicated by folds of decreasing dihedral
angle. The upper diagrams represent anticlines, with cross-sections below the fold line. Likewise, the lower
diagrams depict the synclines. Except where indicated with strike and dip symbols, the traces represent
vertical planes.
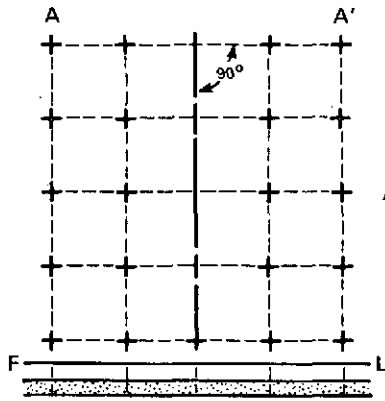
ANTICLINE

SYNCLINE

$\phi = 180°$ $\phi = 150°$ $\phi = 120°$ $\phi = 90°$

25

REFERENCE BED

FRACTURE TRAJECTORY (TRACE OF FRACTURE
PLANE INTERSECTION WITH REFERENCE BED)

TRACE OF FOLD AXIS

21   STRIKE AND PLUNGE OF TRAJECTORY

▲ 60   STRIKE AND DIP OF FRACTURE PLANE

ϕ DIHEDRAL ANGLE OF FOLD

F———L   FOLD LINE
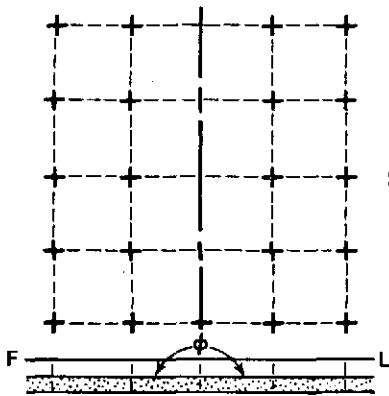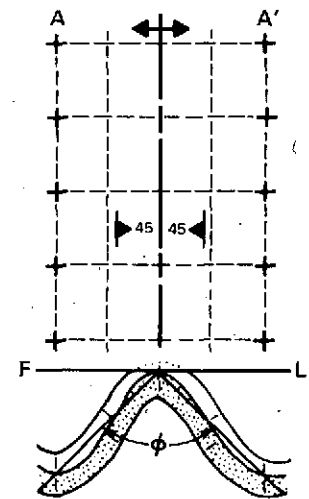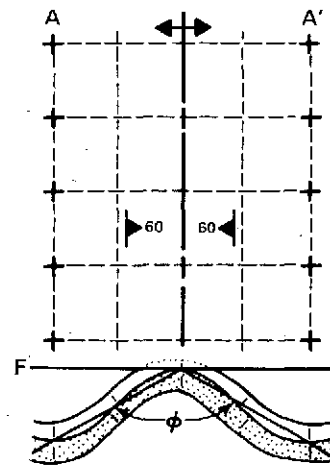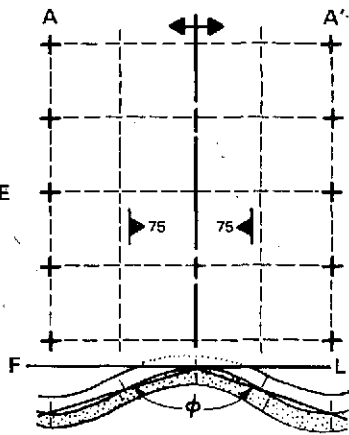
+   VERTICAL FRACTURE PLANE INTERSECTION
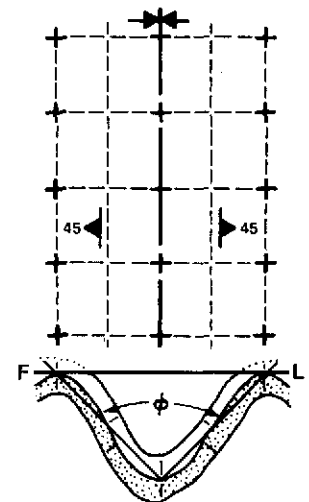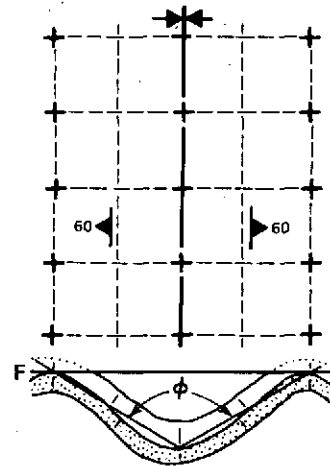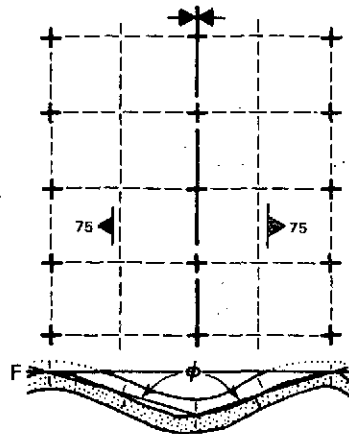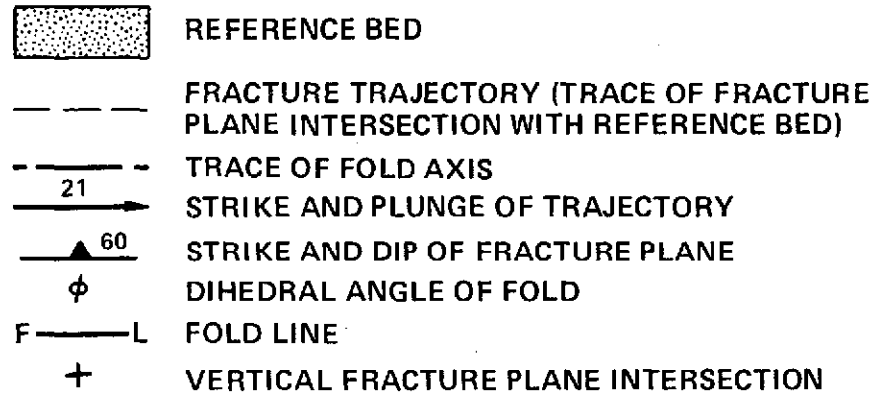
Figure 6. Plan view of trajectories of an original square, vertical fracture grid projected vertically from its intersection with the top of the folded reference bed. The initial state is shown on the left with the square grid oriented 45° and 315° to the fold axis. Progressively increasing deformation is indicated by folds of decreasing dihedral angle. The upper and lower diagrams respectively represent anticlines and synclines, and both sets are served by the same cross-sections (to view synclinal case, turn page 180°). Fractures are warped out of the vertical between the crest and trough positions (see Figure 2). The strike and dip of these tangent planes at the mid-point position are given, as well as the plunge of the line of intersection with the reference surface. The trajectories are drawn in by linking the crest, mid-point, and trough positions.

N

ϕ =180

ANTICLINE

SYNCLINE

ϕ = 150°

ϕ = 120°

ϕ =90°

REFERENCE BED

FRACTURE TRAJECTORY (TRACE OF FRACTURE
PLANE INTERSECTION WITH REFERENCE BED)

TRACE OF FOLD AXIS

21   STRIKE AND PLUNGE OF TRAJECTORY

▲60   STRIKE AND DIP OF FRACTURE PLANE

ϕ DIHEDRAL ANGLE OF FOLD

F——L   FOLD LINE
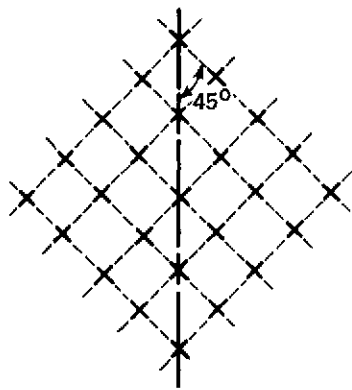
+   VERTICAL FRACTURE PLANE INTERSECTION
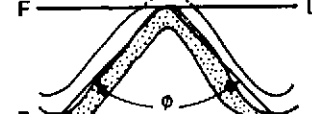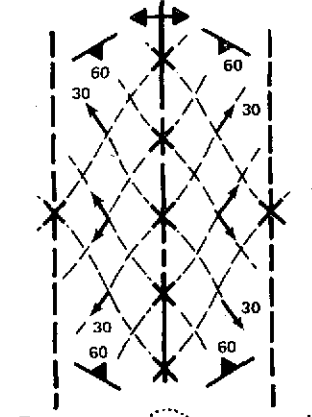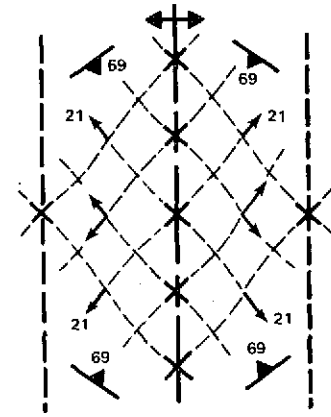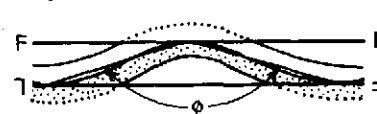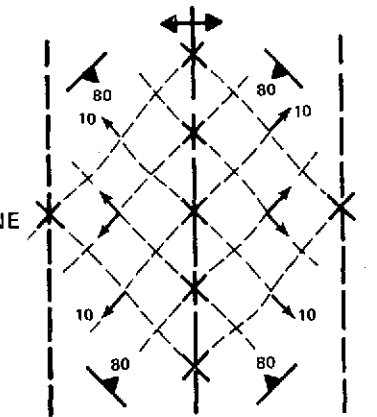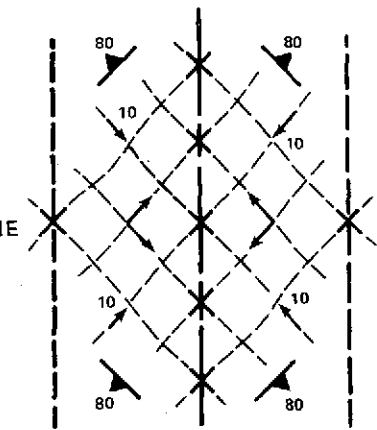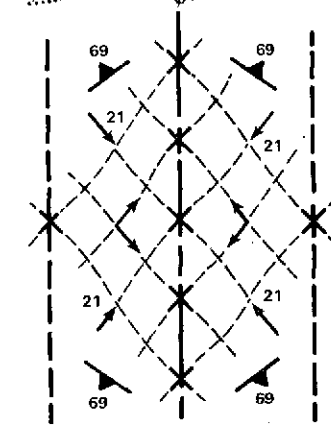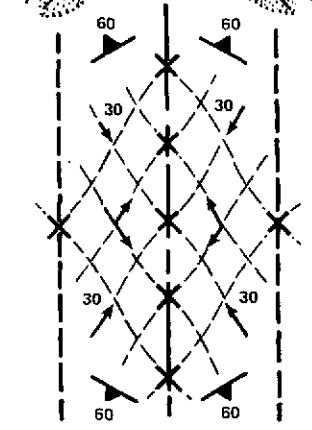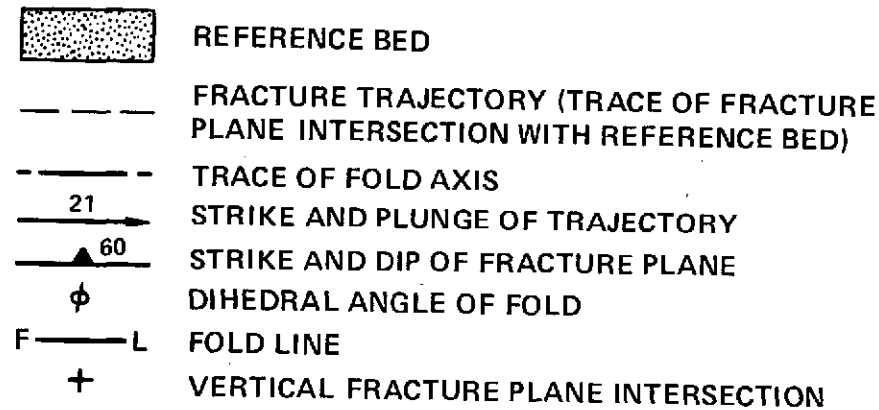
Figure 7. Plan view of trajectories of an original square, vertical fracture grid projected vertically from its intersection with the folded reference bed. The initial state is shown on the left with the square fracture grid oriented 30° (330°) and 300° (60°) to the fold axis. Progressively increasing deformation is indicated by folds of decreasing dihedral angle. The upper and lower diagrams respectively represent anticlines and synclines, and both sets are served by the same right sections (as per Figure 6). Fractures are warped out of the vertical between the crest and trough positions, and their attitudes are indicated by the strike and dip of their tangent planes at the mid point positions, as well as the plunge of the line of intersection with the reference surface. The trajectories are drawn in by linking the crest, mid-point, and trough positions.

ANTICLINE

SYNCLINE

N

30°
60°

60°
30°

$\phi = 180°$

$\phi = 150°$

$\phi = 120°$

$\phi = 90°$

REFERENCE BED

FRACTURE TRAJECTORY (TRACE OF FRACTURE
PLANE INTERSECTION WITH REFERENCE BED)

TRACE OF FOLD AXIS

▲60 STRIKE AND DIP OF FRACTURE PLANE

φ DIHEDRAL ANGLE OF FOLD

F————L FOLD LINE
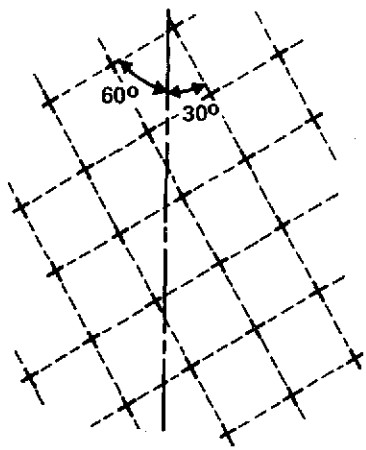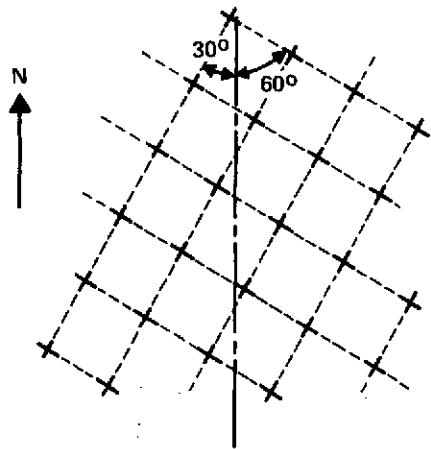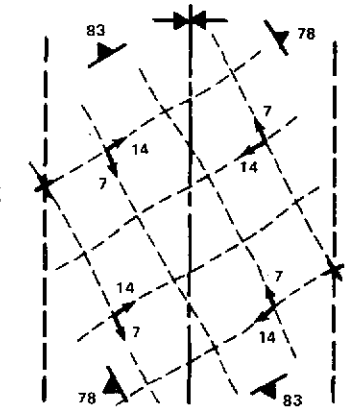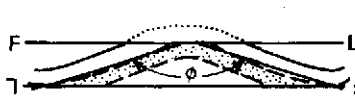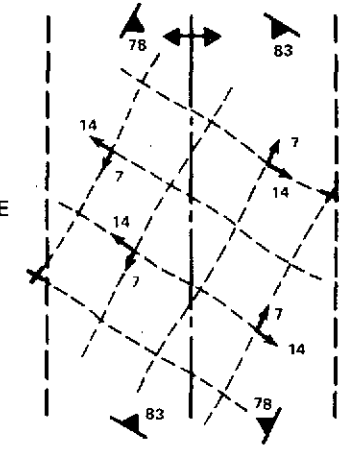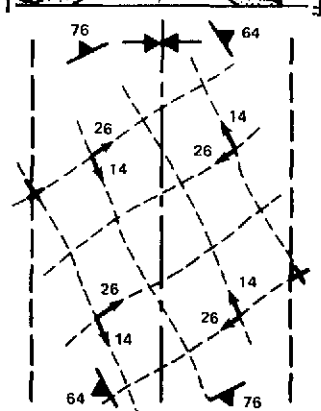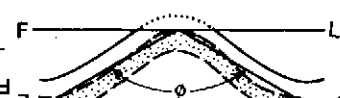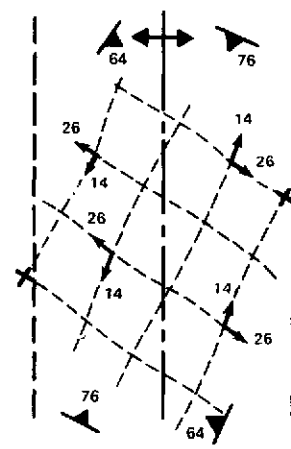
+ VERTICAL FRACTURE PLANE INTERSECTION
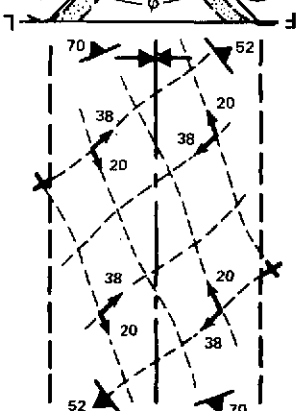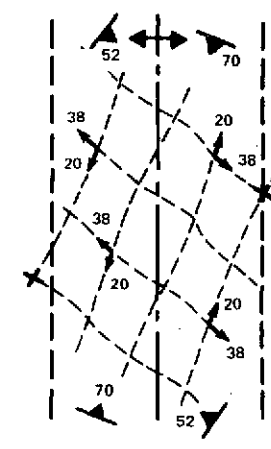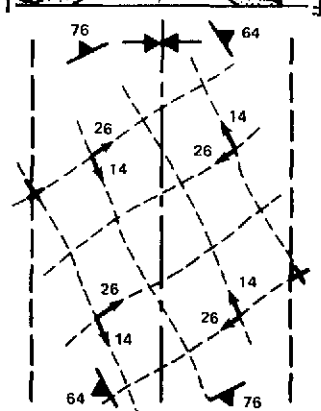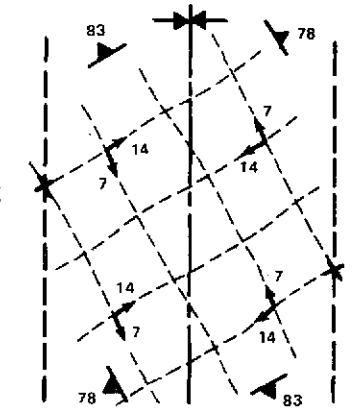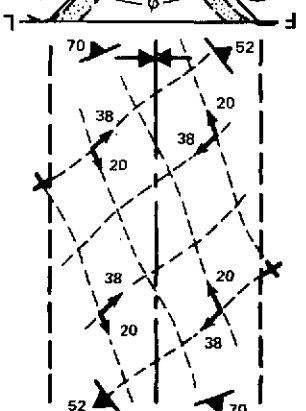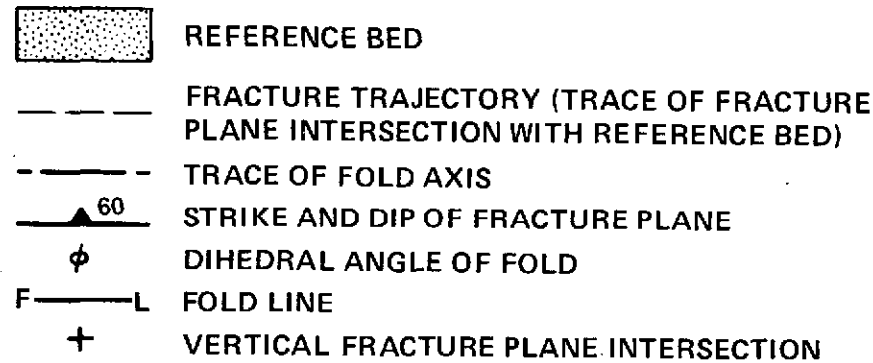
Figure 8. Plan view of trajectories of an original square, vertical fracture grid projected vertically from its intersection with the domed or basined reference bed. The initial state for two sets of grids are shown on the left. The upper and lower diagrams respectively represent domes and basins, and both sets are served by the same cross-sections (as per Figure 6). Progressively increasing deformation is indicated by cones of decreasing apical angle. All fractures are warped out of the vertical, except for those in radial directions from the axis. The strike and dip of tangent planes to some of the fractures are given.

N

DOME

F ——————————— L

F ——————————— L

F ——————————— L

BASIN

φ = 180°   φ = 150°   φ = 120°   φ = 90°

BASEMENT ROCKS

REFERENCE BED

FRACTURE TRAJECTORY (TRACE OF FRACTURE PLANE INTERSECTION WITH REFERENCE BED)

21 STRIKE AND PLUNGE OF TRAJECTORY

60 STRIKE AND DIP OF FRACTURE PLANE

F————L FOLD LINE

+ VERTICAL FRACTURE PLANE INTERSECTION
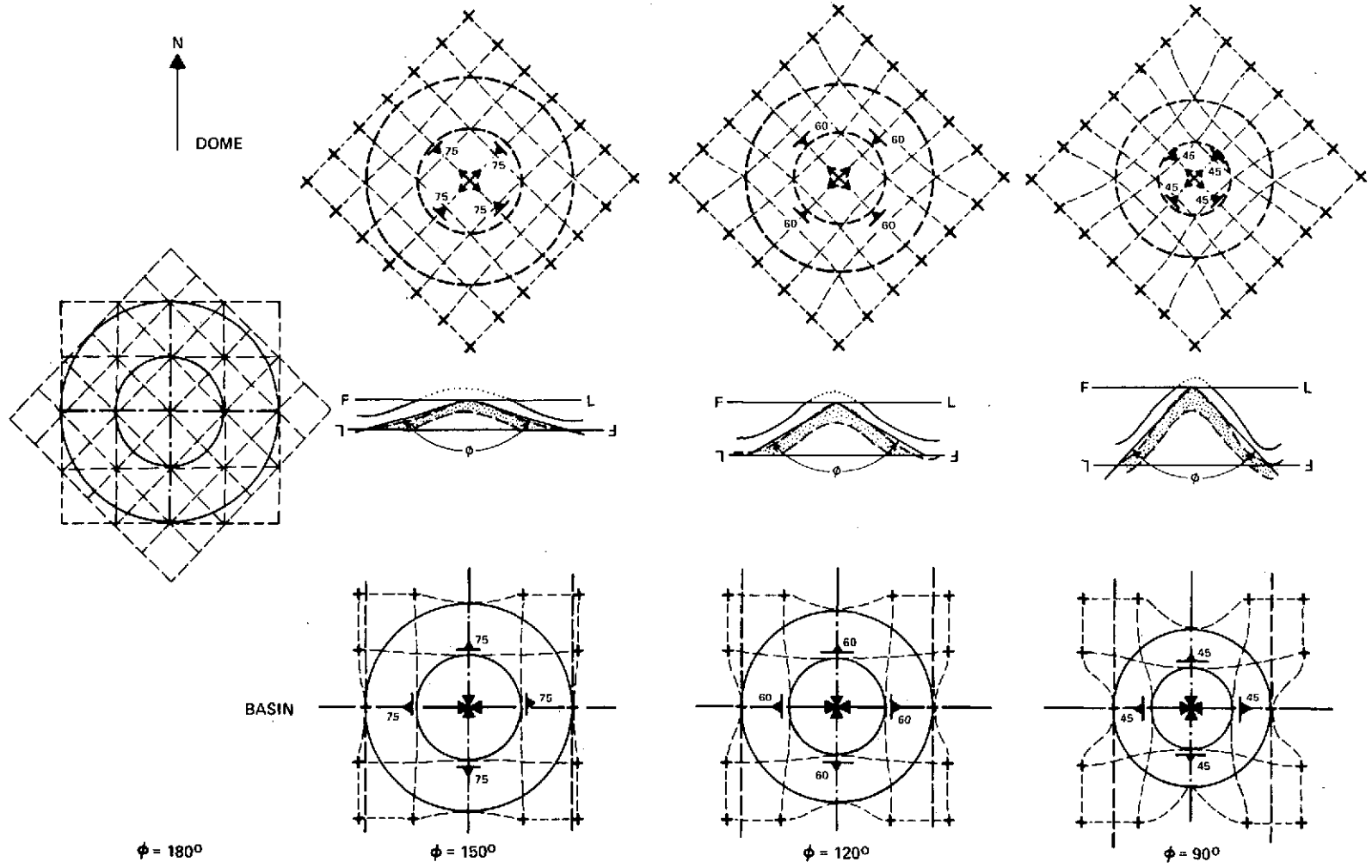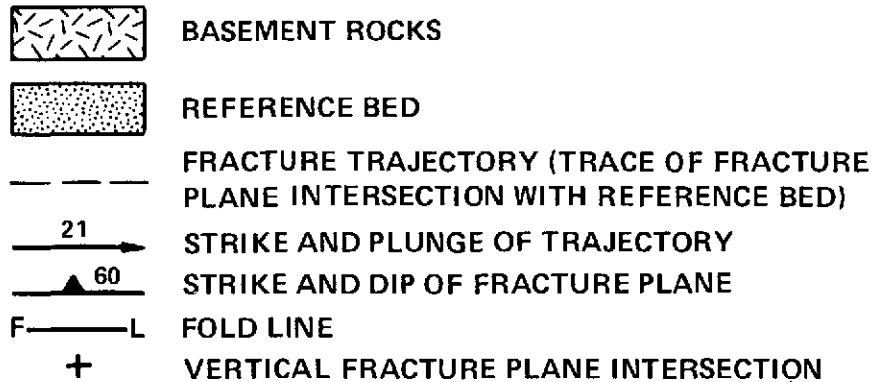
Figure 9. Diagrams illustrating possible fracture trajectories from a reference bed involved in monoclinal structures with dips respectively of 45° (Monocline) and 90° (Box Fold).   (a) Cross sections showing progressive draping over a basement block.   (b) Plan view of fracture trajectories for an initial grid oriented 0° and 90° to the monoclinal axis.   (c) Plan view of fracture trajectories for an initial grid oriented 45° and 315° to the fold axis.   (d) Plan view of fracture trajectories for an initial grid oriented 60° and 330° to the fold axis.   Note: for oblique orientations of the grid to a box fold, the strike of the fractures is rotated to a position perpendicular to the fold axis. The dip of the fracture will correspond to its initial angle to the fold axis, and its intersection with the reference bed (trajectory) will coincide with the dip line.

a)

b)

c)

d)

N

MONOCLINE   BOX FOLD

33
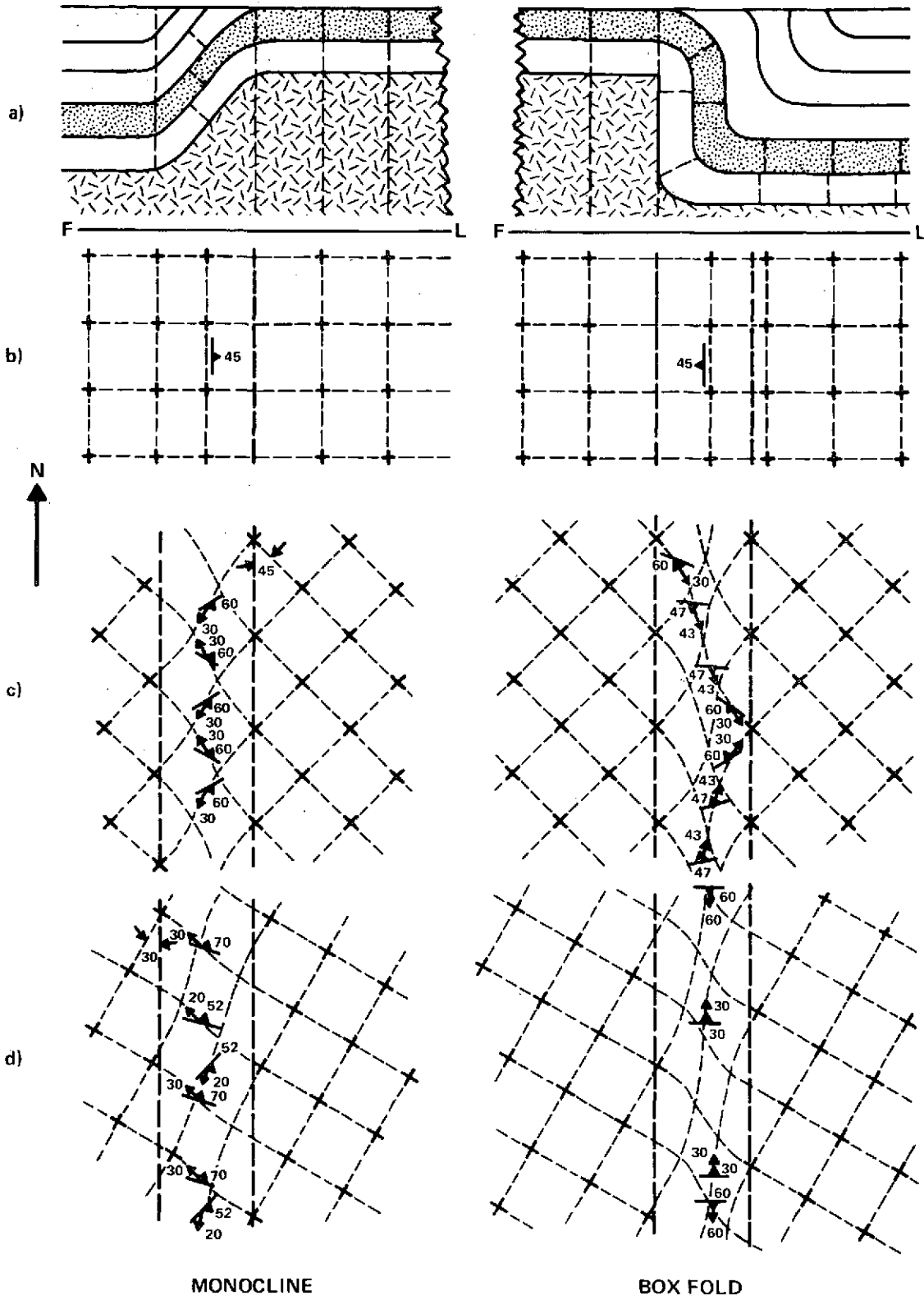
- ———— -	TRACE OF FOLD AXIS
▲60	STRIKE AND DIP OF FRACTURE PLANE
ϕ	DIHEDRAL ANGLE OF FOLD; $\phi = 150°$
F————L	FOLD LINE
+	VERTICAL FRACTURE PLANE INTERSECTION
O	REFERENCE SURFACE
1-4	LEVELS OR DATA PLANES
A	CENTER OF TROUGH CURVATURE
B	CENTER OF RIDGE CURVATURE

Figure 10. Diagrams illustrating fracture patterns projected gnomonically from a line through a grid on a reference surface. The cross-sections of a trough and ridge (upper diagrams) show radial fracture lines intersecting different levels. A strip representing each level is drawn in plan view in the lower diagrams with the two fracture grids, respectively 0-90° (solid lines) and 45-315° (dashed lines) superimposed. All lines in these lower diagrams represent directly the fracture intersections on the earth's surface.

LEVEL OR DATUM PLANE

CROSS SECTION VIEW

PLAN VIEWS

ORIGINAL

35

— — —   FRACTURE TRAJECTORY (TRACE OF FRACTURE
        PLANE INTERSECTION WITH REFERENCE BED)

___▲60___ STRIKE AND DIP OF FRACTURE PLANE

   ✛   VERTICAL FRACTURE PLANE INTERSECTION
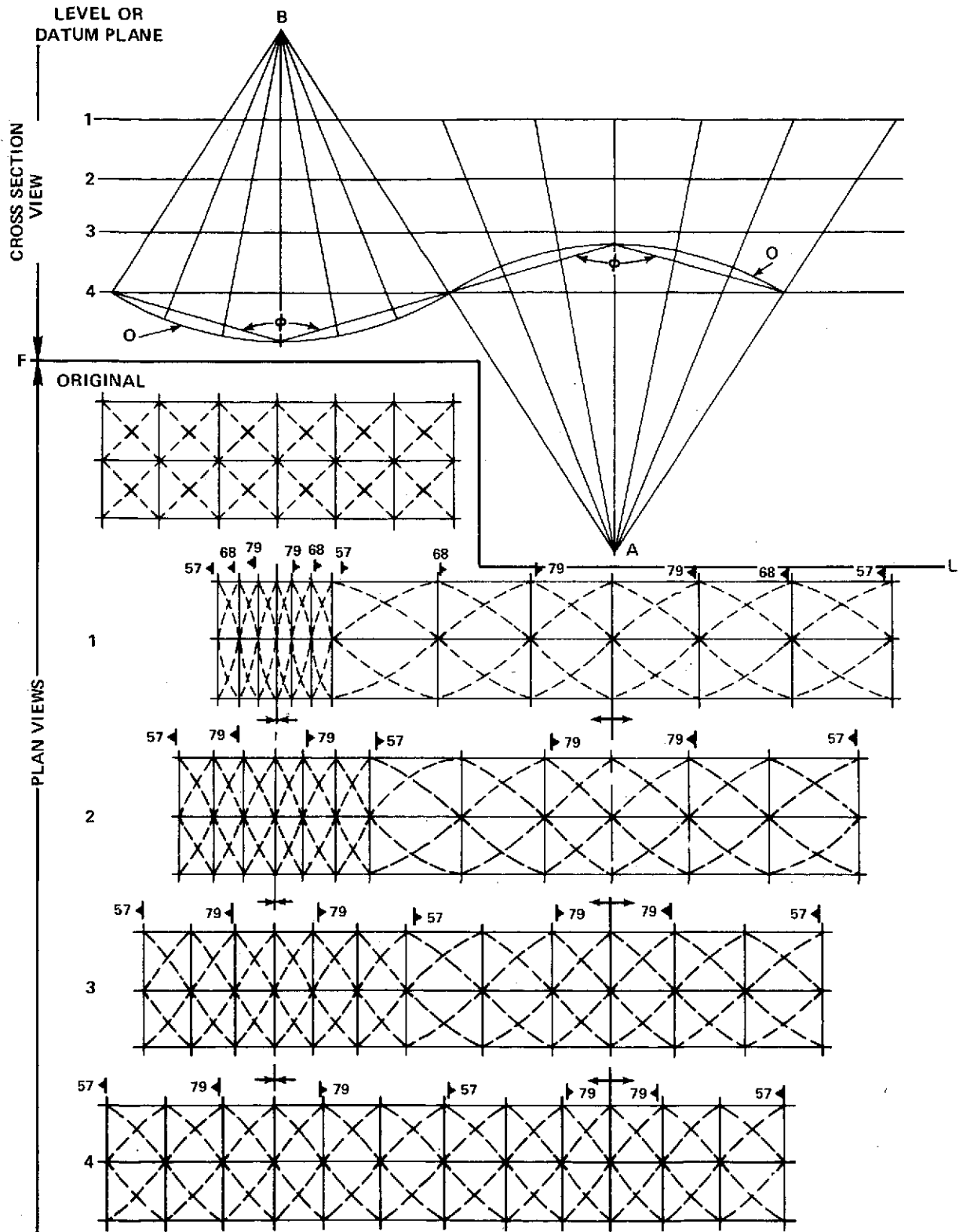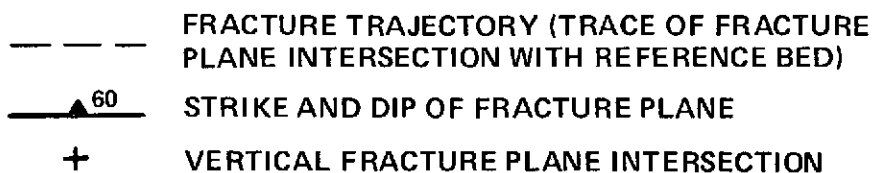
Figure 11. Diagrams illustrating a fracture pattern projected
gnomonically from a point through a grid on a spherical ref-
erence surface. (a) Plan view of the orthogonal grid on top of
a spherical unconformity surface (dome portion of level 0 in
Figure 10). (b) Map view of the grid pattern as it would
appear on a surface at level 3. Diagrams for other levels
are not given, but they would represent more extreme distor-
tions than are depicted for level 3. The concentric circles
represent the outline of the subsurface dome and/or basin
projected gnomonically to the surface; they may also repre-
sent the pattern of concentric fractures developed during
compaction.

(a)

BASIN   DOME

(b)

37
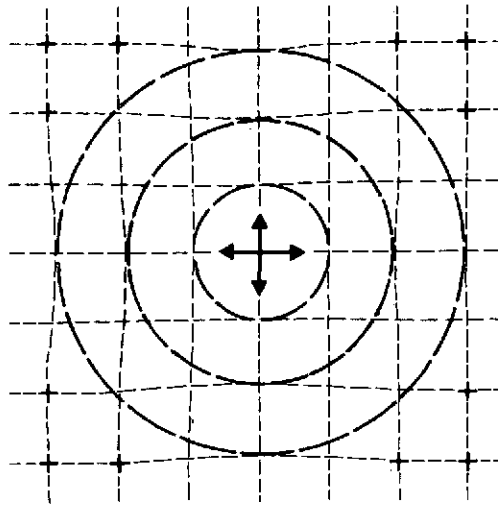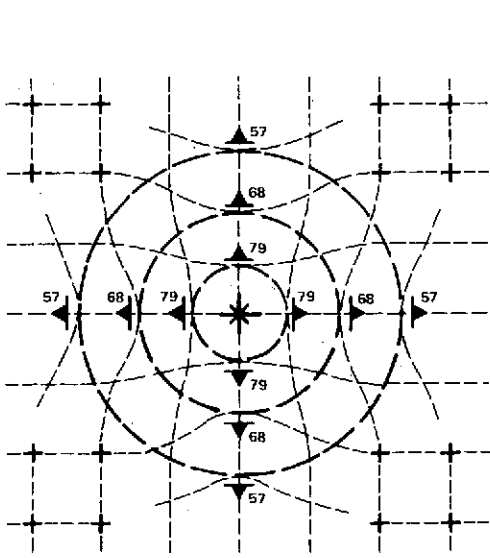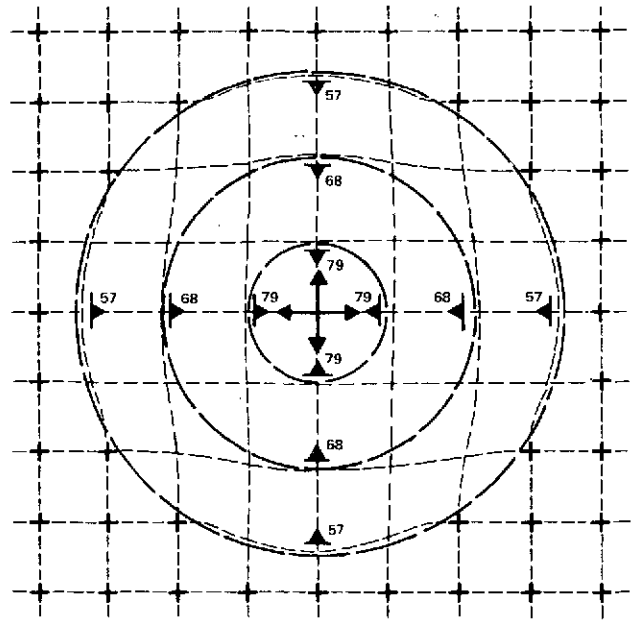
Table 1

Post-Deformational Orientations of a Pre-Exisiting Orthogonal Grid Pattern at Various Angles to a North-Trending Fold Axis (or Dome) for Different Culmination (Dihedral) Angles

Fold Dihedral[1] or Apical Angle	Initial Grid[1] Trend	Post Deformation on Flank	
		Fracture Plane[1,2] (Strike/Dip)	Trajectory[1,3] (Inclination/Trajectory)
150	000	000/75	0/000
	090	090/90	15/090
120	000	000/60	0/000
	090	090/90	30/090
90	000	000/45	0/000
	090	090/90	45/090
60	000	000/30	0/000
	090	090/90	60/090
30	000	000/75	0/000
	090	090/90	75/090
0	000	000/0	horizontal
	090	090/90	vertical
150	045	046/80	10/044
	315	213/80	10/136
120	045	050/69	21/041
	315	210/69	21/139
90	045	055/60	30/036
	315	305/60	30/144
60	045	064/53	38/028
	315	296/53	38/152
30	045	075/47	43/015
	315	285/47	43/165
0	045	090/45	45/000
	315	090/45	45/180
150	030	031/78	7/029
	300	299/83	14/121
120	030	034/64	14/027
	300	296/76	26/124
90	030	039/52	20/022
	300	292/70	38/129
60	030	050/41	26/015
	300	286/65	49/138
30	030	066/34	29/008
	300	279/62	57/160
0	030	090/30	30/000
	300	090/60	60/180

[1] All values in degrees.

[2] Direction of fracture plane dip will depend upon the limb of the fold. On the eastern limb of an anticline, the inclined fractures will generally dip toward the west.

[3] The sense of the trajectory plunge will depend upon the fold considered. The values given are for the eastern limb of an anticline and also correspond to the western limb of a syncline. For the opposite limb, add 180° to the trajectory direction.